

# High aspect ratio InGaAs FinFETs with sub-20 nm fin width

Alon Vardi, Jianqiang Lin, Wenjie Lu, Xin Zhao and Jesús A. del Alamo

Microsystems Technology Laboratories, Massachusetts Institute of Technology (MIT), Cambridge, MA 02139, U.S.A  
alonva@mit.edu

## Abstract

We demonstrate self-aligned InGaAs FinFETs with sub-20 nm fin width fabricated through a CMOS compatible front-end process. Working devices with fins as narrow as 7 nm, fin aspect ratios in excess of 5 and gate lengths as short as 20 nm have been fabricated using precision dry etching and digital etch. The devices also feature self-aligned metal contacts that are 20-30 nm away from the edge of the gate. FinFETs with  $L_g=30$  nm,  $W_f=22$  nm and channel height of 40 nm exhibit a transconductance of 1400  $\mu\text{S}/\mu\text{m}$  at  $V_{DS}=0.5$  V. When normalized to  $W_f$ , this is a record value among all III-V FinFETs, indicating that our device architecture makes efficient use of conduction along the fin sidewalls.

## Introduction

InGaAs is a promising candidate as channel material for CMOS technologies beyond the 10 nm node [1]. In this dimensional range, only high aspect-ratio (AR) 3D transistors with a fin or nanowire configuration can deliver the necessary performance. Impressive fin and nanowire based InGaAs FinFET prototypes have recently been demonstrated [2-4]. However, to date, InGaAs FinFETs with fin widths below 30 nm and channel aspect ratio better than unity have yet to be demonstrated. Furthermore, the channel sidewall slopes demonstrated so far are typically lower than 80°. At the point of insertion in a sub-10 nm node, InGaAs FinFETs with sub-10 nm fin widths and steep sidewalls will be required.

In this work, we present the first self-aligned InGaAs FinFETs with sub 20-nm fin width, high channel aspect ratio, vertical sidewalls, gate lengths as short as 20 nm and CMOS-type manufacturability. For this, we use a top down process based on a combination of RIE and digital etch. Our transistors are the most aggressively scaled InGaAs FinFETs to date.

## Process Technology

Our fabrication process closely follows CMOS requirements, particularly self-alignment of the refractory metal gate and metal contacts, very low thermal budget, gate-last process that uses RIE extensively and an entirely lift-off free process in the front end.

The starting heterostructure is shown in **Fig. 1**. It is grown by MBE and it features a  $H_c=40$  nm thick InGaAs channel layer and an  $n^+$  InGaAs cap. The process is illustrated in **Fig. 2** and follows a flow developed for self-aligned planar InGaAs Quantum-Well MOSFETs [5]. SEM images of sub-20 nm fin test structures are shown in **Fig. 3**. **Figs. 4-5** show SEM images of FinFETs at different steps in the process.

Low-p Mo is first sputtered as contact metal ( $R_{sh}=5 \Omega/\square$ ), followed by  $\text{SiO}_2$  CVD. The gate pattern is defined by E-beam lithography. The  $\text{SiO}_2$  and Mo layers are then etched by RIE. After RIE mesa isolation, the top  $n^+$  InGaAs cap is wet-etched in a well-controlled manner that yields an undercut of ~20 nm (**Fig. 4**). Fins are then patterned using 40 nm thick HSQ and E-beam lithography and RIE etched using a  $\text{BCl}_3/\text{SiCl}_4/\text{Ar}$  chemistry [6]. This yields fins as narrow as 20 nm with an  $H_f/W_f$  (**Fig. 2**) aspect ratio of 8. The fins are highly vertical in the top ~70 nm (**Fig. 3**). To further thin down the fins and

smooth the sidewalls, we perform digital etch cycles [7].

Immediately after the last digital etch cycle, 0.5 nm of  $\text{Al}_2\text{O}_3$  and 2.5 nm  $\text{HfO}_2$  are deposited by ALD (EOT~1 nm). Sputtered Mo is used as gate metal and patterned by RIE. The device is finished by via opening and pad formation. This is the only lift-off step at the backend of the process. The final gate length is defined by the recess opening in the  $\text{SiO}_2$  which can reach below 20 nm. In this process, the HSQ that defines the fin etch is kept in place. This makes our FinFETs double-gate transistors with carrier modulation only on the sidewalls.

## Transistor Results

The electrical characteristic of a device with  $W_f=22$  nm and  $L_g=600$  nm are shown in **Fig. 6**. Well-behaved long-channel characteristics and good sidewall control are obtained. **Fig. 7** shows electrical characteristics of a  $W_f=22$  nm (AR=  $H_c/W_f=1.8$ ),  $L_g=30$  nm device. Its  $R_{on}$  is  $180 \Omega\cdot\mu\text{m}$  and a peak  $g_m$  of 1400  $\mu\text{S}/\mu\text{m}$  is obtained at  $V_{DS}=0.5$  V. This value is comparable to the highest  $g_m$  obtained so far in InAs FinFETs with  $W_f=40$  nm (AR=0.23) [8]. The subthreshold characteristics of our device indicate a subthreshold swing,  $S$ , of 170 mV/dec and DIBL of 220 mV/V at 0.5 V (**Fig. 8a**). **Fig. 8b** shows the subthreshold and output characteristics of the most aggressively scaled device obtain in this work with  $W_f=7$  nm (AR=5.7) and  $L_g=20$  nm. Well behaved characteristics are demonstrated. Consistent with the double-gate nature of our devices, all figures of merit have been normalized by two times the channel height.

## Discussion

**Fig. 9** shows  $R_{on}$  as a function of  $L_g$  for different  $W_f$ .  $R_{sd}\sim 100 \Omega\cdot\mu\text{m}$  for all  $W_f$  is obtained. This excellent value emerges from the self-aligned design. **Fig 10** shows  $V_T$  (1  $\mu\text{A}/\mu\text{m}$  at  $V_{DS}=50$  mV) as a function of  $L_g$  for different  $W_f$ . While for  $W_f=22$  and 17 nm a classic  $V_T$  rolloff is observed, for  $W_f=12$  nm a strong dependence over the entire  $L_g$  range is visible. We attribute this to line edge roughness which affects thin long fins [9]. This effect is also enhanced due to quantum size effects [10].  $g_{m,\max}$ ,  $S$ , and  $I_{on}$  as a function of  $L_g$  for different  $W_f$  are shown in **Fig. 11**. A clear tradeoff between  $g_m$  and  $S$  emerges, which governs the  $L_g$  at which maximum  $I_{on}$  (at a fixed  $I_{off}=100 \text{nA}/\mu\text{m}$  and  $V_{DD}=0.5$  V) is obtained. As the fins become narrower,  $I_{on}$  peaks at shorter  $L_g$  while  $g_{m,\max}$  and  $S_{min}$  also degrade. We attribute this is to the increased effect of sidewall scattering and suggests further work is needed.

As a benchmark of our results, **Fig. 12** shows peak  $g_m$  normalized to the fin width as a function of  $W_f$  for InGaAs FinFETs from the literature and our own. This FOM emphasizes the importance of maximizing current drive in very thin fins. Our InGaAs FinFETs are the first to feature sub-30 nm  $W_f$  and they also exhibit the highest  $g_m$  per fin footprint to date.

## Conclusions

We demonstrate the first self-aligned InGaAs FinFETs with  $W_f<30$  nm and channel aspect ratio as high as 6. Fully operational devices with fin widths as narrow as 7 nm and sub-30 nm gate lengths are demonstrated. A record  $g_m$  per fin footprint has been achieved.

**Acknowledgment:** This work was partially funded by DTTRA (HDTRA 1-14-1-0057), NSF E3S STC (grant #0939514) and Lam Research. Device fabrication was carried out at MTL and EBL at MIT. Thanks to Dr. Doron Cohen-Elias for useful discussions.

**References:** [1] J. A. del Alamo, *Nature*, 479, 317 (2011). [2] M. Radosavljevic et al., *IEDM* 2011, p. 765. [3] T-W. Kim et al., *IEDM* 2013, p. 415. [4] A. Thathachary et al., *VLSI* 2015. [5] J. Lin et al., *IEDM* 2013, p. 421. [6] X. Zhao et al., *IEDM* 2013, p. 695. [7] J. Lin et al., *EDL* 35(4) 440 (2014). [8] S-H Kim et al., *TED* 61(5), 1354 (2014). [9] J. B. Chang, *VLSI* 2011. [10] A. Vardi et al., *IEDM* 2015, p. 807.



Fig. 1: Starting heterostructure.

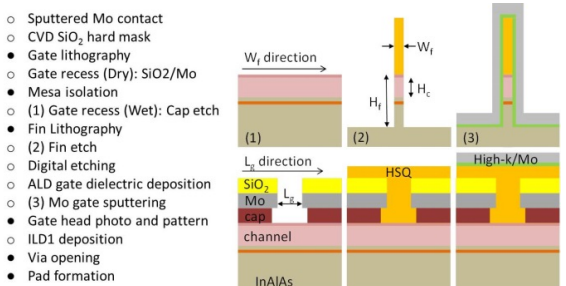


Fig. 2: Left: process flow. Right: device schematics at the points in the process marked by numbers.

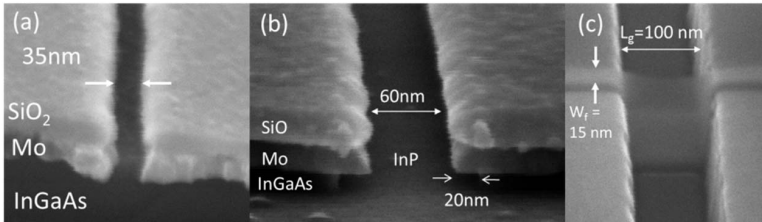


Fig. 4: SEM images of transistors in process: (a) after dry recess, (b) after wet recess, and (c) after fin etch.

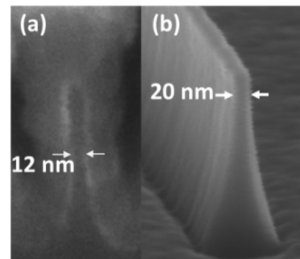


Fig. 3: InGaAs fins in this work: (a) cross-section, (b) stand alone.

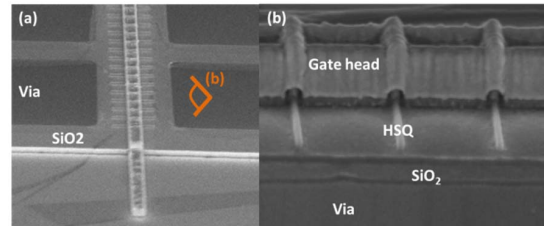


Fig. 5: SEM images from back end after gate patterning and via opening. (b) view marked in (a).

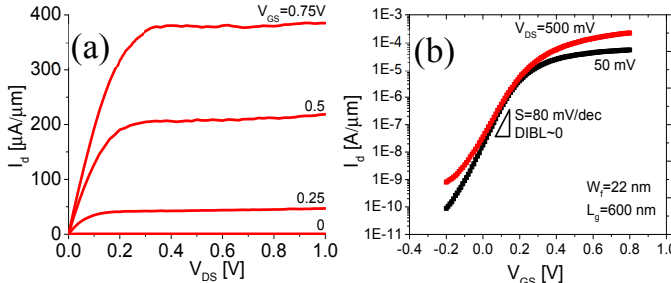


Fig. 6: Output (a) and subthreshold (b) characteristics of FinFET with  $W_f=22$  nm and  $L_g=600$  nm.

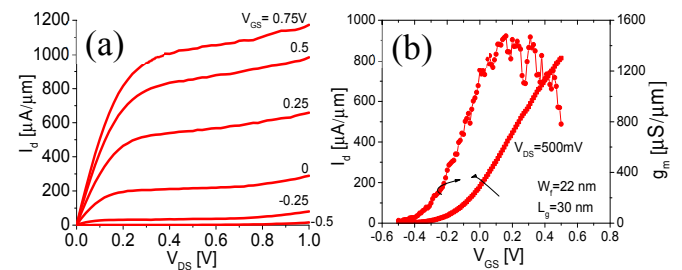


Fig. 7: Output (a) and transfer (b) characteristics of device with  $W_f=22$  nm and  $L_g=30$  nm.

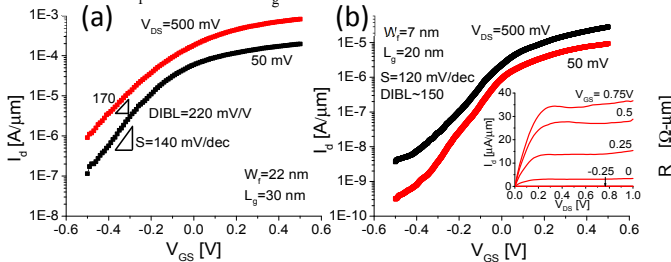


Fig. 8: Subthreshold characteristics of (a)  $W_f=22$  nm,  $L_g=30$  nm and (b)  $W_f=7$  nm,  $L_g=20$  nm devices. Inset of (b): output characteristics of the same device.

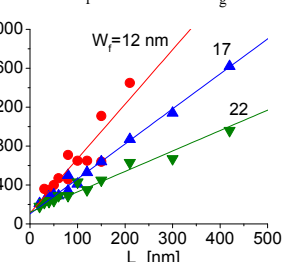


Fig. 9:  $R_{on}$  as a function of  $L_g$  for different  $W_f$ .

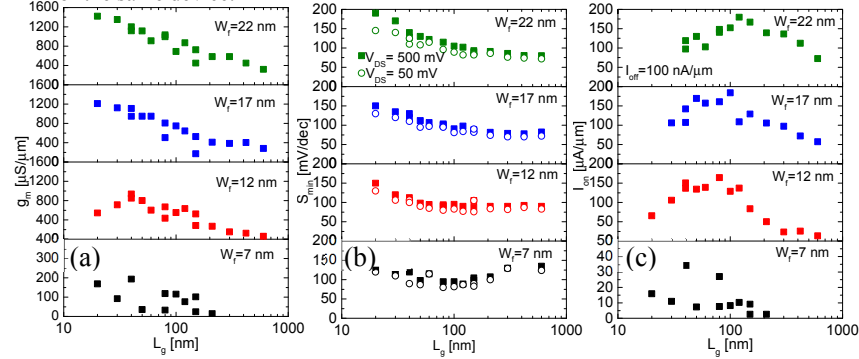


Fig. 11: From left to right:  $g_m$  at  $V_{DS}=0.5$  V,  $S_{min}$  (linear and saturated), and  $I_{on}$  (at  $I_{off}=100$  nA/ $\mu\text{m}$  and  $V_{DD}=0.5$  V) as a function of  $L_g$  for different  $W_f$ .

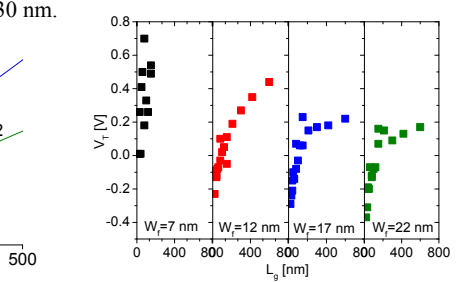


Fig. 10:  $V_T$  at  $1 \mu\text{A}/\mu\text{m}$  and  $V_{DS}=50$  mV as a function of  $L_g$  for different  $W_f$ .

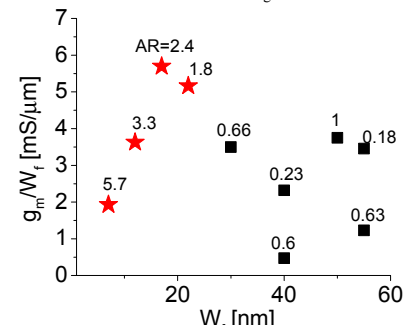


Fig. 12: Benchmark of  $g_m$  per fin footprint vs.  $W_f$  for InGaAs FinFETs in the literature (black squares) and this work (red stars). Each data point is labeled with the channel AR= $H_c/W_f$ .